Magneto-optical study of interface mixing in the CdTe-(Cd,Mn)Te system

J.A. Gaj,* W. Grieshaber, C. Bodin-Deshayes, and J. Cibert
Laboratoire de Spectrométrie Physique, Université Joseph Fourier, Grenoble I, Boîte Postale 87, 38402 Saint Martin d'Hères, France

G. Feuillet
Département de Recherche Fondamentale–Matière Condensée, Centre d'Etudes Nucléaires de Grenoble, Boîte Postale 85, 38041 Grenoble, France

Y.Merle d'Aubigné and A. Wasiela
Laboratoire de Spectrométrie Physique, Université Joseph Fourier, Grenoble I, Boîte Postale 87, 38402 Saint Martin d'Hères, France
(Received 8 February 1994; revised manuscript received 19 May 1994)

We present in detail a quantitative description of Zeeman splittings of exciton states in a nonmagnetic quantum well with diluted-magnetic-semiconductor barriers which takes interface mixing into account. For structures with high Mn concentration in the barrier we show that this effect leads to a dramatic increase of the Zeeman splitting even to a value exceeding the barrier splitting. We describe a method of interface characterization based on Zeeman-effect measurements. It enables one to study the shape of the interface profile, the influence of the growth conditions on the interface, and provides a perspective to decouple the influence of interface mixing from truly two-dimensional magnetic effects in studies of ultrathin magnetic layers. The influence of the parameters of the model on the results obtained and the practical applicability of the method are discussed. In particular we show that the quantum-well profile is strongly asymmetric in relation to the growth direction and we demonstrate the small influence of the intrinsic effect related to interface magnetism.

I. INTRODUCTION

A great deal of effort has been invested recently in developing efficient methods for studying the structure of semiconductor-semiconductor interfaces, both experimentally[1–7] and theoretically.[8] Interface roughness has been studied by means of photo[1,2] and cathodoluminescence,[3] Raman scattering,[2,4] electron transport,[5] soft x-ray reflectivity,[6] and high-resolution electron microscopy.[7] Each of these methods has its own scale for the observation of the interface roughness spectrum. For example, luminescence related methods use excitons created in quantum-wells and therefore are directly sensitive to the roughness on a scale comparable with the effective size of the exciton. Even in the case of high-energy transmission electron microscopy, which, especially when complemented by a thorough numerical analysis,[7] seems to supply the most faithful image of the interface structure, some doubts remain because the method integrates over the thickness of the studied layer; in addition, it is destructive.

Successful growth of molecular-beam-epitaxy (MBE) layers and structures involving diluted magnetic semiconductors[9] (DMS) has opened a whole area of new phenomena such as magnetic field induced type I–type II transitions[10] or spin superlattices.[11,12] Precise knowledge of the interface of two-dimensional (2D) DMS structures is important in understanding the physics of these structures. In particular, the wide spread of the values of the valence band offset in the $CdTe/Cd_{1-x}Mn_xTe$ system published so far, attributed by some authors to interface effects, calls for a quantitative explanation. Interface studies of DMS systems may also contribute to the understanding of mechanisms of interface formation in MBE, fundamentally important for the development of new electronic and photonic devices.

In this paper we develop a recently proposed[13] method of studying interfaces between a DMS and a nonmagnetic semiconductor, based on measurements of Zeeman splittings of exciton states localized in a nonmagnetic quantum well with DMS barriers. Diluted magnetic semiconductors are known for their giant magneto-optical effects, occurring via alignment of magnetic ions in an external magnetic field.[14] A carrier (exciton) in a nonmagnetic quantum well with DMS barriers appears to be a perfect tool for interface studies: a magnetic field will not influence it greatly within the well (where there are no magnetic ions) or deep in the barriers (where the carrier does not penetrate) but precisely in the neighborhood of the interface. To illustrate the possibilities of the method, we present some experimental data obtained on suitable MBE grown structures.

We start from a description of the sample growth and experimental procedure, followed by a qualitative discussion of experimental results; we show the main model-independent conclusions which can be obtained at this stage: the necessity of introducing interface mixing to explain the observed strong enhancement of the Zeeman

effect in structures with large concentration ($x > 20\%$) of Manganese in the barriers, small role of intrinsic interface magnetic effects, and a strong asymmetry of the quantum-well profile. In Sec. IV we discuss the origin of the interface broadening, interdiffusion, segregation, roughness, and the method of describing it by a potential profile. We also introduce the strain corrections to the band offsets. In Secs. V and VI we present the quantitative study of the interface effects and describe various aspects of the model: choice of the valence band offset, of the composition profile, and contribution of the intrinsic surface magnetic effect. In Sec. VII we discuss various factors influencing the precision of our description: possible uncertainty of the quantum-well width, direct Zeeman effect, variation of the exciton binding energy with magnetic field, and use of a continuous concentration profile. Finally in Sec. VIII we discuss applications of the Zeeman effect as a method of interface characterization and present graphs allowing us to obtain a rapid estimation of intermixing range in $CdTe/Cd_{1-x}Mn_xTe$ quantum-wells.

II. SAMPLES AND EXPERIMENT

Samples were grown by MBE on (001) $Cd_{1-x}Zn_xTe$ substrates with $x = 4$–12%, using three effusion cells to provide adapted nonstoichiometric fluxes: CdTe, Mn, and Cd. A Zn cell allowed us to incorporate $Cd_{1-x}Zn_xTe$ layers in samples M336 and M340. Growth temperature was varied between 250 °C and 310 °C. Alloy compositions were adjusted using reflection high-energy electron diffraction (RHEED) intensity oscillations on a test sample; they were checked afterwards through low temperature reflectivity. We use for the free exciton energy (in meV) versus Mn mole fraction of $Cd_{1-x}Zn_xTe$ the expression

$$E_{ex}(Cd_{1-x}Mn_xTe) = E_{ex}(CdTe) + E_x \ , \qquad E_{ex}(CdTe) = 1596 \ , \quad E_x = 1563x \ . \tag{1}$$

Slightly different values have been proposed for the slope (e.g., $E_x = 1592x$ in Ref. 9). The only significance of this dependence (taken from an unpublished part of the results of Ref. 14) for this work is to parametrize the energy gap of the barriers: in fact the important parameter in the analysis is not the exact alloy composition x, but the energy change E_x of the exciton, which defines the depth of the quantum well, and the Zeeman splitting in the alloy, which is experimentally measured as a function of E_x (Sec. V B), and E_x is measured directly on the sample under study. The actual composition of the alloy is needed only for rather small corrections (lattice mismatch effect, interface magnetic correction, etc., see; below): in these cases we use $x \approx E_x/1563$, but the exact value of the slope dE_x/dx is not necessary. The thickness of quantum-wells was measured through RHEED oscillations (for 001 growth direction, molecular layer width equals 3.24 Å for unstrained CdTe). Sample M097 comprises two CdTe quantum wells QW1 and QW2 (thickness 5.5 and 20 monolayers, respectively) with thick $Cd_{0.68}Mn_{0.32}Te$ barriers. Growth was interrupted in the vacuum for a few seconds at each interface. The structure was grown without a $Cd_{1-x}Mn_xTe$ buffer on a thin CdTe layer, which was deposited first in order to smooth the surface. The sample temperature was rapidly decreased immediately after the growth of the last barrier, so that the two quantum-wells were kept at 310 °C only for a few minutes. Samples M162, M177, and M178 are representative of a larger series of samples which were grown to study the influence of growth temperature on interface mixing. Each of them contains a 20 monolayer quantum well. Samples M336 and 340 belong to a series of samples which have been grown to check whether the quantum-well profile is symmetric or not. They contain CdTe quantum wells with two different barriers: one magnetic ($Cd_{1-x}Mn_xTe$) and one nonmagnetic ($Cd_{1-x}Zn_xTe$). The principal difference between the two samples is related to the growth direction: in sample M340 the magnetic barrier was grown after the CdTe quantum well, while in the sample M336 the order is opposite. In all the samples the substrate (buffer) lattice constant and thickness of the deposited layers have been chosen to assure pseudomorphic growth of the structures. Parameters of the samples are collected in Table I.

Magnetoreflectivity measurements were performed in the Faraday configuration with samples mounted strain-free in a 5 T superconducting magnet. Samples were immersed in superfluid helium. Photoluminescence was excited with an argon ion laser providing typically 2–20 mW over a spot of diameter between 0.1 and 2 mm. The zero-field reflectivity and photoluminescence spec-

TABLE I. Parameters of the samples. Lengths in Å, energies in meV, temperatures in 6 °C. For simulations, an exponential profile and $\alpha = 0.4$ were used. Letter M in the samples' names indicates Mn content.

Sample	QW width		$Cd_{1-x}Mn_xTe$ barriers			$Cd_{1-x}Zn_xTe$ bar		Intermed.	Growth	Growth	$Cd_{1-x}Zn_xTe$ comp.	
name	Nominal	Adjusted	x	E_x	Width	x	Width	length	temp.	interrupt.	Substrate	Buffer
M097	17.8	17.0	0.32	504	> 300	none		5.6	310	5s	0.04	none
	64.8	65.8						6.1		5s		
M162	64.8	72.5	0.23	383	> 300	none		6.6	310	none	0.04	none
M177	64.8	63.4	0.24	375	> 300	none		4.4	280	2 min	0.04	none
M178	64.8	61.2	0.22	336	> 300	none		3.1	250	2 min	0.04	none
M336	46.7		0.35	559	19.2	0.112	73.3	4.7	280		0.12	0.11
M340	43.2		0.32	509	18.6	0.117	75.5	see text	280		0.12	0.12

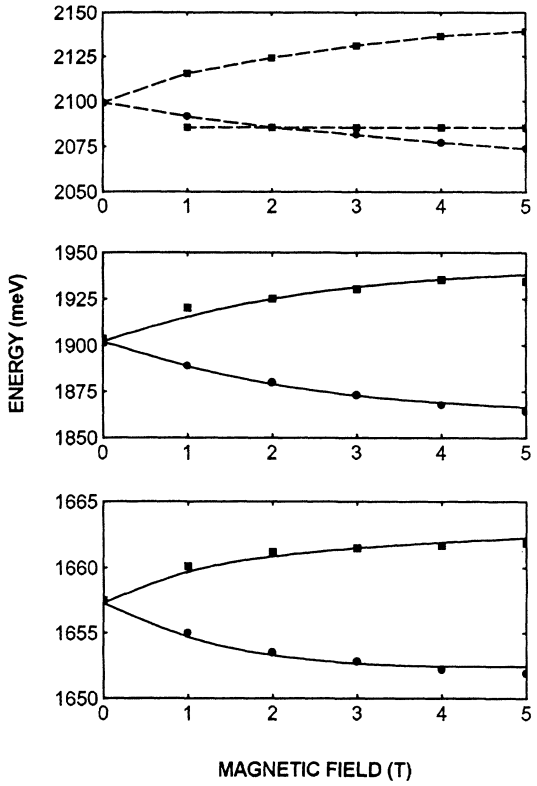

FIG. 1. Energy of magnetoreflectivity structures corresponding to exciton ground states in the barrier and in both quantum-wells of sample M097, plotted versus magnetic field. Circles: σ^+ polarization, squares: σ^- polarization. Continuous lines: model described in text; dashed lines added to guide the eye.

tra obtained on sample M097 have been shown in Ref. 13 (Fig. 1). We identify the two most intense luminescence lines as related to heavy hole ground state (e^1h^1) excitons of both quantum wells. The two corresponding reflectivity structures as well as the barrier free exciton reflectivity structure are marked by arrows. The influence of a magnetic field on the reflectivity spectrum is presented in Fig. 1. Barrier data allow us to determine the uniaxial stress in the barriers from the heavy hole–light hole splitting (hidden in the line width at zero magnetic field). On the basis of that splitting (14 meV) we calculate the uniaxial stress in the CdTe layer equal to the one expected assuming pseudomorphic growth. Thus the strain in both $Cd_{1-x}Mn_xTe$ and CdTe layers is well defined.

III. EXPERIMENTAL RESULTS AND A QUALITATIVE DISCUSSION

This section describes experimental results obtained on samples of Table I, which can be qualitatively understood, and will help in choosing the right approximations for the quantitative interpretation. In particular, they demonstrate the necessity of introducing interface mixing, the fact that the two interfaces of a QW are very different, and give an upper limit to intrinsic magnetic effects at a sharp interface.

Figure 1 reveals an interesting fact: the Zeeman splitting of the exciton localized in a nonmagnetic QW1 is larger than that of the barrier exciton, in spite of the fact that the influence of the magnetic field is mediated by the Mn^{++} ions, present only in the barrier. This result shows clearly that a natural approximation, in which the ratio of the quantum-well state splitting to the barrier splitting measures the probability of the presence of the exciton in the barrier,[15] is completely useless. A better description, commonly used to describe similar structures, expresses quantum-well Zeeman splittings as a spin-dependent variation of the confinement energy,[16] resulting from a strong variation of barrier heights in the magnetic field. Such a description cannot explain the observed splitting values either. Two principal physical mechanisms can be responsible for the enhancement of the quantum well Zeeman splittings: interface mixing and/or intrinsic magnetic interface effects. The idea of the interface mixing in CdTe/(Cd,Mn)Te system[17,18] and its role as a source of difficulties in a quantitative description of the Zeeman effect in DMS 2D structures[19] has already been discussed by several authors. Magneto-optical measurements on excited states of excitons in quantum wells have been proposed[20] to determine interdiffusion in a CdTe/$Cd_{1-x}Mn_xTe$ structures. Other authors attach primary importance to particular magnetic properties of thin layers[21] or intrinsic magnetic properties of the near-interface region in semimagnetic semiconductors.[22] It is well known that in alloys such as $Cd_{1-x}Mn_xTe$ with large x the paramagnetism is strongly reduced by the short range exchange interaction between the Mn spins.[9] Thus the Mn spins sitting at the CdTe interface having less Mn neighbors should exhibit a larger magnetization than the spins lying deeper inside the $Cd_{1-x}Mn_xTe$ layer.

Experiments performed on samples M336 and M340 containing quantum wells with only one magnetic barrier supply very interesting data related to these problems. Figure 2, representing Zeeman shifts of the quantum well exciton ground state in both samples, shows a striking difference between the Zeeman splittings: 1.4

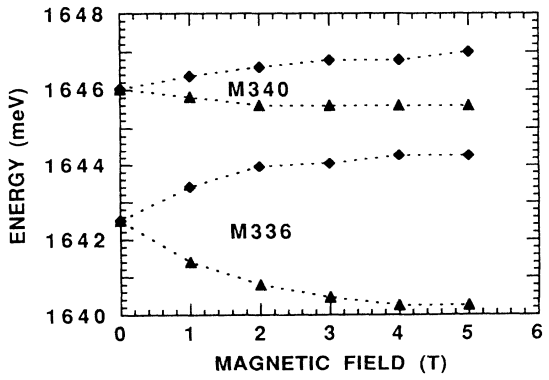

FIG. 2. Energy of e^1h^1 magnetoreflectivity structures of samples M336 and M340, plotted versus magnetic field. The dotted curves are guides for the eye.

meV at 5 T in M340 vs 4.5 meV in M336. These results show clearly two facts: first, the normal ($Cd_{1-x}Mn_xTe$ on CdTe) interface is very different from the inverted (CdTe on $Cd_{1-x}Mn_xTe$) one; second, the intrinsic magnetic interface effect alone without a broadening of the interface cannot be responsible for the observed Zeeman splitting values, since it would be the same for both samples. Furthermore, since the smaller of the two splittings (sample M340) constitutes an upper bound for the contribution of the intrinsic magnetic interface effect to the Zeeman splitting, we see that this effect introduces a small contribution to the Zeeman splitting measured on sample M336 and, most probably, for any comparable quantum well with both barriers containing magnetic ions. We can conclude at this stage that the above experimental facts confirm our explanation given in Ref. 13, that the principal reason of the observed enhancement of the Zeeman splittings is the facility with which ions in the broadened interface can align with the magnetic field, acquired by dilution. We shall proceed to a quantitative analysis of these phenomena in the following sections.

IV. CdTe/$Cd_{1-x}Mn_xTe$ INTERFACE

A. Roughness, interdiffusion, and segregation

As pointed out in the preceding section, in order to explain the experimental facts we need a dilution of magnetic ions at the interface leading to a decrease of ion-ion exchange interaction (the latter being of very short range[23]). Such an effect would not occur if the interface imperfection had the form of long range roughness (Fig. 3), as in the case of the rather broad islands usually encountered in the GaAs-$Ga_{1-x}Al_xAs$ system at the normal interface ($Ga_{1-x}Al_xAs$ on GaAs). Then only the atoms at the step edges have a number of metallic neighbors which differ from those at the flat interface, and this should make a small contribution, smaller indeed than the interface magnetic corrections which will be evaluated later on. However, it is well known that the inverted interface (GaAs on $Ga_{1-x}Al_xAs$) has fluctuations on a shorter scale, due to the usually smaller diffusion of the Al atoms at the growing $Ga_{1-x}Al_xAs$ surface: such a mechanism in the CdTe-$Cd_{1-x}Mn_xTe$ system would result in an enhanced Zeeman effect at the inverted interface CdTe-on-$Cd_{1-x}Mn_xTe$. We should mention that roughness has been measured by high-resolution transmission electron microscopy on MnTe layers, so that the CdTe-on-MnTe interface broadens as the thickness of the MnTe layer increases, while the MnTe-on-CdTe interface remains sharp;[24] this was observed, however, at growth temperatures where no RHEED intensity oscillations could be recorded for MnTe, which indeed suggests that roughness develops. On the contrary RHEED oscillations were observed during the growth of the present $Cd_{1-x}Mn_xTe$ samples. While the long-scale roughness is not of concern here, the short-scale roughness can be represented in the model we develop, and cannot be excluded in the CdTe-$Cd_{1-x}Mn_xTe$ structures.

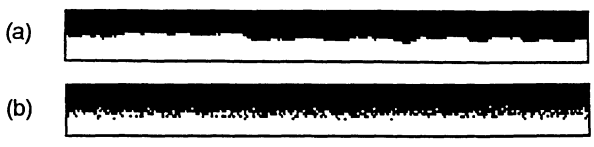

FIG. 3. Schematic images of interface broadening effects: (a) roughness, (b) intermixing.

Another source of dilution of the magnetic ions is a possible interdiffusion at the interface: this is easily represented by a dilution profile in a continuous description. In Ref. 13 we used an error function profile identical at both interfaces, corresponding to bulk-type interdiffusion: this description will be fully adapted to studies of after-growth annealing. Significant interdiffusion is observed upon annealing of CdTe-$Cd_{1-x}Mn_xTe$ structures, but at temperatures higher that those used during growth, or for longer times. In as-grown structures a clear asymmetry of the quantum-well profile is evidenced by the experiments performed on samples M336–M340. Such an asymmetry could result in a surface enhanced diffusion: one would then have to assume that defects diffuse from the surface through the thin CdTe layer to enhance interdiffusion at the CdTe-on-$Cd_{1-x}Mn_xTe$ interface, and that the diffusion of the same defects is slower in the $Cd_{1-x}Mn_xTe$ layer. The resulting profile would have to be described in our model using functions similar to the previous one (bulk diffusion), but with a different width at each interface. A quite similar profile should also describe the effect of a depletion in Mn at the short growth interruption usually realized at the interface. We have measured such a depletion over up to more than ten monolayers during interruptions of the $Cd_{1-x}Mn_xTe$ growth under a Cd flux: if the effect exists when the growth is interrupted in the vacuum, or even during the formation of the first CdTe layer, it is smaller than under Cd flux, but difficult to exclude.

Segregation (or more generally exchange of Cd/Mn atoms between the last incorporated monolayer and the surface layer) naturally results in asymmetric profiles: the easiest way to represent it is an exponential function. If we assume an excess of Mn at the growing $Cd_{1-x}Mn_xTe$ surface, as is observed for In in the growth of $G_{1-x}In_xAs$,[25] for compositions around 20–30% the magnetic dilution will be more efficient at the inverted interface (where Mn progressively incorporates at a large dilution in the growing CdTe) than at the normal one (where the alloy will be only a little bit more diluted than expected). This asymmetry is very well represented in the following model.

The above mentioned cases of dilution at the interface are easily described in a continuous model. However, the discrete nature of the interface can also play a role. The difference between the continuous model and the discrete one in the preceding cases is negligible, as will be shown later in the paper. However, a continuous model cannot be developed if only one monolayer is concerned at the interface. This is the case if the interface width is due to the fact that the beam shutters were activated during 2D growth while the last monolayer was not completed. If surface diffusion is large enough the surface will reorga-

nize to form broad islands, one-monolayer thick, with no enhancement of the Zeeman effect. However, if surface diffusion is small in the extreme case the single monolayer at the interface can be described as an alloy with a reduced Mn content. A similar profile should exist if the surface reconstruction corresponds to an incomplete surface layer (this is indeed the case of the $c(2\times 2)$ surface of CdTe, for which the topmost layer is a half-filled Cd layer[26]). If this is realized on a short scale, then on switching from one material to the other only a fraction of the sites remain available and the one monolayer at the interface will have a smaller Mn content. This kind of profile can be described in the model, see the end of Sec. VII.

Finally, we also have to keep in mind the possibility of different local magnetic properties at a perfect abrupt interface, due to the reduced number of magnetic neighbors at the interface as compared to bulk. We shall call this intrinsic effect "interface magnetic corrections" in the following. The description of a truncated disordered magnetic system is difficult, and it seems that even the range of these corrections (strictly local or over a correlation range) is not obvious and could depend on the magnetic structure of the alloy, hence on the composition, the temperature, and the applied field. The present model directly correlates the local magnetization and the local composition, but it can be slightly modified to incorporate separately the chemical profile and the magnetization profile: this is done in the last part of Sec. VI under the assumption that the magnetization depends on the local composition and on the composition of the neighboring atomic planes.

To sum up, to separate ions from their neighbors we need a roughness or a dilution on the atomic scale. This makes us choose a continuous model, which can encompass several causes of interface broadening, although most examples in the following will be given for the special profile adapted to segregation. But we must remember that the Zeeman effect will give us little information on medium and large scale interface roughness. Those will contribute to the overall quality of the sample and influence such parameters as line width and photoluminescence Stokes shift. Therefore, to obtain complete information about the interface, it is desirable to combine different methods of interface characterization. These interesting problems will be treated in a forthcoming publication, devoted to the influence of the growth conditions on the quality of MBE grown structures.

B. Interface profile

According to the above remarks, we shall represent the interface mixing by a continuous variation of the composition across the interface. Any variation in the interface plane will be neglected. Let us introduce an interface profile function $P(z)$. It is convenient to represent it as a convolution of the perfect (step) profile with a broadening function $g(z)$:

$$P(z)=\int_{-\infty}^{+\infty} g(u)\Theta(z-u)\,du\ ,$$

where Θ is the Heaviside step function. It is easy to see that the broadening function $g(z)$ is simply the derivative of the profile function $P(z)$. For example, if we choose for $P(z)$ an erf function, $g(z)$ will be the corresponding Gaussian function. We normalize these functions in such a way that the zeroth moment (integral) and the second moment, if it exists (z^2 mean value), of the $g(z)$ function are equal to 1 and choose the z origin to make the first moment vanish. In the case of long range profiles, where the second moment diverges, the scale of the z axis must be chosen otherwise (arctg profile in Table II). We shall then have of course $P(-\infty)=0$ and $P(\infty)=1$.

Using the above definitions we may express the variation of the crystal composition across the interface from $x=0$ to $x=x_0$ in the form $x(z)=x_0P(z/l_0)$, where l_0 is the rms intermixing length. For a CdTe quantum well of width w between barriers of Mn mole fraction x_0 the composition profile will be

$$x(z)=x_0P_{\mathrm{QW}}(z,w,l_0)\ , \tag{2}$$

where $P_{\mathrm{QW}}(z,w,l_0)=P\left(\frac{z-w/2}{l_0}\right)-P\left(\frac{z+w/2}{l_0}\right)+1$ is the quantum-well profile.

A few examples of profile functions are collected in Fig. 4 and Table II. The actual width of the interface is defined by l_0; for example, in the case of diffusion (e.g., annealing for a time t at a temperature where the diffu-

TABLE II. Examples of interface profiles.

Profile name	Profile function	Generating function	Remarks
linear	$P(z)=\begin{cases}\frac{z+\sqrt{3}}{2\sqrt{3}} & \lvert z\rvert<\sqrt{3}\\ \Theta(z) & \lvert z\rvert\geq\sqrt{3}\end{cases}$	$g(z)=\begin{cases}\frac{1}{2\sqrt{3}} & \lvert z\rvert<\sqrt{3}\\ 0 & \lvert z\rvert\geq\sqrt{3}\end{cases}$	extreme short tail
error function	$P(z)=\mathrm{erf}(z)$	$g(z)=\frac{1}{\sqrt{2\pi}}\exp\left(-\frac{z^2}{2}\right)$	diffusion case
exponential	$P(z)=\begin{cases}\exp(z-1) & z<1\\ 1 & z\geq 1\end{cases}$	$g(z)=\begin{cases}\exp(z-1) & z<1\\ 0 & z\geq 1\end{cases}$	segregation case
acr tangent	$P(z)=\frac{1}{\pi}\arctan\left(\frac{z}{\pi}\right)+\frac{1}{2}$	$g(z)=\frac{\pi^2}{\pi^2+z^2}$	extreme long tail; rms range infinite

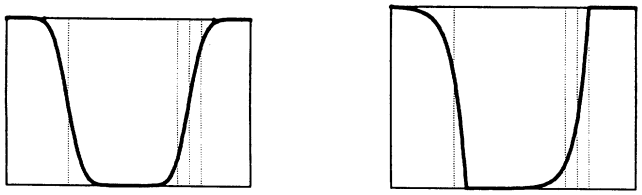

FIG. 4. Examples of quantum-well potentials with various interface profiles. Quantum-well width equal to ten units of intermixing range. (a) Error function; (b) exponential profile.

sion coefficient is D), the function $g(z)$ is Gaussian and $l_0 = (2Dt)^{1/2}$. Unless stated otherwise, for the calculations performed in this work we use the exponential profile.

C. Band offsets

In order to calculate potentials for electrons and holes we have to divide the barrier-well band gap difference between the conduction and the valence band. We shall denote by α the valence band offset of $Cd_{1-x}Mn_xTe$ relative to the band gap difference,

$$\alpha = \frac{E_v(\mathrm{CdTe}) - E_v(\mathrm{Cd_{1-x}Mn_xTe})}{E_g(\mathrm{Cd_{1-x}Mn_xTe}) - E_g(\mathrm{CdTe})} .$$

There is no consensus on its value in the CdTe/$Cd_{1-x}Mn_xTe$ system. Numbers from almost zero[16] to 0.46[27] have been published. The idea of interface effects being responsible for these discrepancies is beginning to be accepted among the physicists involved.[18,28] We shall discuss this problem in detail later. For most of our calculations, following Ref. 18, we choose $\alpha = 0.4$. Various simulations show that the essence of the conclusions reached in this paper remain valid if we choose a smaller value of the valence band offset, e.g., 0.3.

The definition of α, which does not take into account the strain effect on the band edges, gives what is sometimes called "chemical offsets." In real structures they must be corrected for strain effects. The deformation potentials of CdTe have been given by several authors[29] and elastic coefficients by Greenough and Palmer.[30] P. Maheswaranathan *et al.*[31] have found elastic constants of $Cd_{1-x}Mn_xTe$ not very different from those of CdTe. Assuming the same deformation potential also for $Cd_{1-x}Mn_xTe$, we obtain strain corrections to the band offsets proportional to the difference of strains in the two materials,

$$\Delta\epsilon_{\|} = \epsilon_{\|}(\mathrm{Cd_{1-x}Mn_xTe}) - \epsilon_{\|}(\mathrm{CdTe}),$$

which is equal to the lattice parameter mismatch of the two materials ($\epsilon_{\|}$ is the in-plane strain), independently of the average strain in the structure, imposed by the substrate or buffer layer. Using the deformation potentials and elastic coefficients as quoted in Ref. 32, we obtain a "practical formula" for the strain corrections to the conduction, heavy and light hole band offsets (in meV),

$$\delta V_e = -35x_{\mathrm{Mn}}, \quad \delta V_{hh} = 45x_{\mathrm{Mn}}, \quad \delta V_{lh} = -81x_{\mathrm{Mn}} .$$

On the other hand, the CdTe energy gap obviously depends on the lattice parameter of the substrate (or of the buffer if its thickness is large enough). For a $Cd_{1-x}Zn_xTe$ substrate (a $Cd_{1-x}Mn_xTe$ buffer layer) with zinc (manganese) concentration x_{Zn} (x_{Mn}), the strain correction to the CdTe energy gap is given by $\delta V_g = -25$ meV x_{Zn} or $\delta V_g = -10$ meV x_{Mn}.

V. MODEL OF QUANTUM WELL WITH INTERFACE MIXING

In this section we describe in detail the model which is used to describe the effect of a diffuse interface quantitatively. Without external magnetic field, see Sec. V A, we just have to solve the Schrödinger equations for the envelope functions of electrons and heavy holes, where the potential profile is calculated by combining Secs. IV B and IV C above. In the presence of a magnetic field, see Sec. V C, the potential profile is obtained by adding, to the zero-field potential of each spin component of each carrier, the Zeeman shift experimentally observed for bulk material with a uniform composition x equal to the local composition $x(z)$. Hence it is necessary to have an accurate numerical representation of bulk Zeeman shifts for any composition, which is given in Sec. V B.

A. Zero field case

Let us first consider a quantum well of width w without magnetic field. For a single carrier (electron or hole) the Schrödinger equation for the envelope function will have the form

$$\left\{-\frac{\hbar^2}{2m}\frac{d^2}{dz^2} + V(z) - E\right\}\Psi(z) = 0 . \tag{3}$$

It is generally recognized that the gap variation as a function of Mn mole fraction in $Cd_{1-x}Mn_xTe$ is linear (see Sec. II). Then, taking into account also strain effects, the potential of the quantum well is proportional to the composition profile

$$V(z) = \gamma x(z)\frac{dE_g}{dx} , \tag{4}$$

where dE_g/dx is given by Eq. (1) and $\gamma = \alpha + \delta V_{hh}/(dE_g/dx)$ for the heavy hole and $\gamma = (1-\alpha) + \delta V_e/(dE_g/dx)$ for the electron. It follows from Eqs. (2) and (4) that $V(z)$ can be written as

$$V(z) = \gamma x_0 P_{\mathrm{QW}}(z, w, l_0)\frac{dE_g}{dx} .$$

We now define natural (carrier-dependent) energy and length units

$$V_0 = \gamma x_0 \frac{dE_g}{dx} \quad \text{and} \quad z_0 = \frac{\eta}{\sqrt{2m_c V_0}} , \tag{5}$$

that is the potential barrier height and the minimum penetration depth of the carrier into the barrier (m_c is the carrier effective mass). Introducing dimensionless reduced energy and length $\epsilon = E/V$ and $\zeta = z/z_0$ we obtain the Schrödinger equation in the simple form

$$\left\{ -\frac{d^2}{d\zeta^2} + P_{\mathrm{QW}}(\zeta, \eta, \lambda) - \epsilon \right\} \Psi(\zeta) = 0 , \tag{6}$$

where η and λ express the well width and the intermixing range in z_0 units.

We see from Eq. (6) that using the above-defined units, we can express the one carrier zero-field energy for a given profile type as a universal (material-independent) function of well width and intermixing length. In Fig. 5 we show this dependence computed for the exponential profile. The influence of intermixing decreases for very small and very large values of the quantum-well width: for the large width, because the intermixing range becomes relatively small, and for the small width, because the energy of the ground state is very close to the barrier height, whatever the intermixing range. The results computed for the error function (erf) function profile are almost identical, except for a small scale change (maximum value equals about 0.23).

Let us point out that the introduced units have a composition dependence ($V_0 \propto x$ and $z_0 \propto x^{-1/2}$) which is the same for electron and hole. Therefore, choosing any common units with this composition dependence, we shall obtain composition-independent Schrödinger equations, one for the electron and one for the heavy hole. Hence for a given material (carrier masses and band offsets) we can compute electron and hole energies and therefore express the interband transition energy as a single function of the quantum-well width and intermixing length, valid for any concentration of magnetic ions in the barrier material. The results calculated for a $CdTe/Cd_{1-x}Mn_xTe$ system using the exponential profile are presented in Fig. 6.

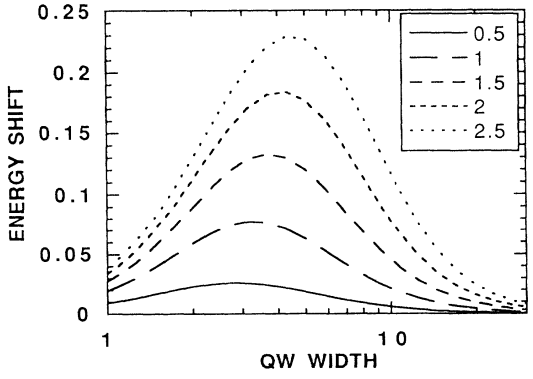

FIG. 5. Eigenenergy shift of a carrier in a quantum well due to interface mixing, plotted versus well width for several indicated intermixing length values l_0. Energy in units of barrier height (i.e., E/V_0), lengths in units of carrier penetration depth [i.e., l_0/z_0 and w/z_0; see text, Eq. (5)]; exponential profile. The figure is in reduced units and material independent.

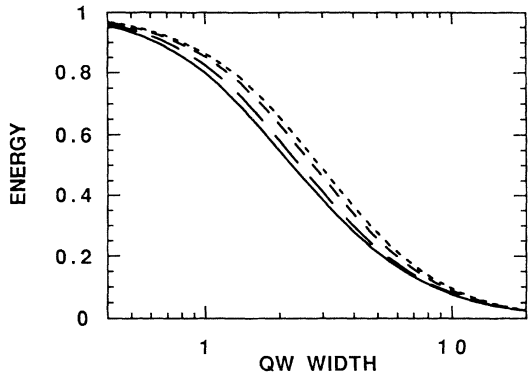

FIG. 6. Sum of the confinement energies of the e^1 and h^1 ground states in $CdTe/Cd_{1-x}Mn_xTe$ quantum-wells as a function of the well width, for four values of the intermixing length (exponential profile). Energy in units of E_x [see Eq. (1)], lengths in units of electron penetration depth z_0 [Eq. (5)]. Relative valence band offset $\alpha = 0.4$. Reduced coordinates allow us to use the plot for any composition of the barrier. Solid line, $l_0/z_0 = 0$; long dashed, 1; dashed, 2; dotted, 2.5.

In order to compare these results with experimental data, it is necessary to know the exciton binding energy. We performed a calculation for the exponential profile and a medium value of intermixing length (4 Å). We used the method developed by Berroir and Bastard and co-workers[33,34] which remains valid at small and/or negative (type II structures) valence band offsets. Using the technique developed by Leavitt and Little[35] we integrate numerically the Schrödinger equation for the relative motion of the electron and hole in the quantum-well potential. This integration is easily performed for any potential profile. Details of the calculation are given in Ref. 32. Using values of Luttinger coefficients from Ref. 36 and dielectric constant $\epsilon = 10.6\epsilon_0$[37] we obtain the results presented in Fig. 7. Having checked that the interface mixing has little influence on the calculated exciton binding energy, we can use Fig. 7 to correct the interband transition energies (Fig. 6) for exciton effects, and compare the results with the measured transition energies. The latter as expected are slightly larger than the

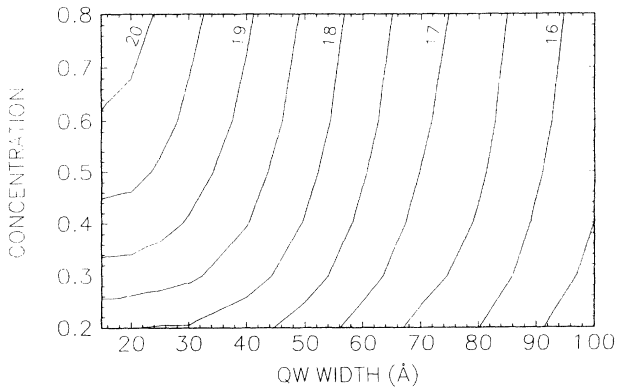

FIG. 7. Binding energy of e^1h^1 excitons calculated as a function of quantum-well width w and barrier Mn mole fraction x. Exponential profile, intermixing length 4 Å.

exciton energy calculated for an ideal quantum well. It would be premature to try to determine the intermixing length at this stage, because of the small sensitivity of the zero-field energy to the interface profile and insufficient precision in the knowledge of some parameter values (well width, band offsets, etc.).

B. Bulk Zeeman splittings

In order to compute the influence of the magnetic field on quantum-well states one has to know the Zeeman splittings of the bands at each point across the interface profile. We shall start from a rough approximation, assuming that Zeeman splittings of the bands in the interface at a point of (local) Mn mole fraction x are equal to those in bulk material of the same x value. This approximation neglects interface magnetic properties resulting from a different number of magnetic neighbors of an ion in the interface, compared to an ion in bulk material of the same composition. We shall return to this problem later.

In order to obtain the bulk Zeeman splitting values, we have performed a series of measurements on MBE layers of (Cd,Mn)Te and used some magnetoreflectivity data obtained by Coquillat and Lascaray[38] on Bridgman grown samples, in the composition range up to $x = 0.67$. The heavy hole exciton splitting as a function of magnetic field can, in our experimental conditions (pumped He temperature, fields up to 5 T), be represented with a good accuracy by a modified Brillouin function[39]

$$\Delta E(B) = \Delta E^s B_J\left(\frac{g\mu_B JB}{k_B(T+T_0)}\right) , \tag{7}$$

where $B_J(x) = \frac{2J+1}{2J}\coth\left(\frac{2J+1}{2J}x\right) - \frac{1}{2J}\coth\left(\frac{x}{2J}\right)$ is the Brillouin function, $J = 5/2$, $g = 2$, μ_B, and k_B are the Bohr magneton and Boltzmann constant, respectively, and T denotes temperature. The two parameters of this description, the saturation value ΔE^s and the temperature shift T_0 have been found to obey the following empirical expressions:

$$\Delta E^s(E_s) = E_x a \exp\left[\left(-\frac{E_x}{b}\right) + c\exp\left(-\frac{E_x}{d}\right) + e\right] \quad \text{and} \quad T_0(E_x) = \frac{fE_x}{1+gE_x} , \tag{8}$$

where $a = 0.4595, b = 36.06, c = 1.272, d = 252.5, e = 0.01258, f = 0.02263$, and $g = 0.001761$. We choose to express the Brillouin function parameters not as functions of alloy composition x, but as functions of bulk free exciton energy related to its CdTe value: [see Eq. (1)]. Experiments of several authors show that the free exciton energy is a linear function of the alloy composition, but slightly different values of the proportionality coefficients are given in various papers. Using a directly measurable value, we get rid of the related uncertainty. The parameter values were obtained by fitting the Zeeman splitting values for 18 samples; the reader may judge the accuracy from Fig. 8, where Zeeman splittings calculated using Eq. (8) are compared to the experimental values. At low x values T_0 and ΔE^s can be determined independently and have a clear meaning in a mean field approximation.[40] However, at high x values, T_0 and ΔE^s become correlated, therefore for $x > 0.2$ one should not pay too much attention to each of them taken separately; our purpose here is to get a reasonably accurate parametrization of the Zeeman splittings.

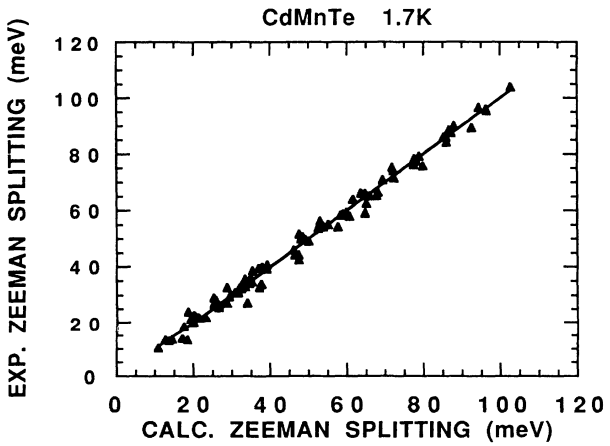

FIG. 8. Experimental values of bulk Zeeman splittings of $Cd_{1-x}Mn_xTe$ free excitons vs the ones calculated using the fit of Sec.V B. Continuous line represents identity.

C. Influence of the Zeeman effect on the band offsets

Using the established empirical description of the bulk Zeeman splittings, and the well known exchange integrals[9] $N_0\beta = 0.88$ eV and $N_0\alpha = 0.22$ eV in the valence and conduction bands, respectively, we determine the magnetic variations of the $\pm 3/2$ heavy holes and of the $\pm 1/2$ conduction band edges as

$$\Delta V(\pm 3/2) = \pm 0.4\Delta E(B)$$

and

$$\Delta V(\pm 1/2) = \pm 0.1\Delta E(B),$$

where $\Delta E(B)$ is the heavy hole exciton Zeeman splitting given by Eq. (7). For example, Fig. 9 shows the variation of the energy of the upper $(-3/2)$ spin component of the heavy hole band edge calculated as a function of magnetic field for several Mn mole fraction values. Adding these variations to the zero-field potential, Eq. (4), we determine one-carrier potentials under applied magnetic field as a function of local alloy composition.

In addition to the quantitative description of interface effects, we can determine from Fig. 9 the field range (if any) for which a type II superlattice will be formed. In

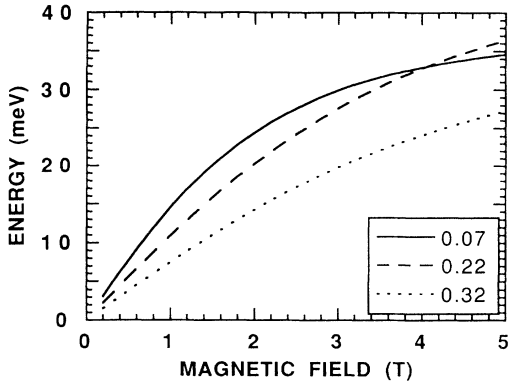

FIG. 9. Zeeman shift of the (−3/2) valence band edge, calculated for several indicated $Cd_{1-x}Mn_xTe$ compositions.

such a manner we determine the type I–type II transition lines in the composition-magnetic field plane, calculated for several assumed values of the valence band offset. Assuming a valence band offset parameter α in the commonly accepted range, 0.2–0.4, for the structures studied in this paper, with manganese compositions of the barriers larger than 0.2, the type I to type II transition is never reached.

VI. DISCUSSION OF PRINCIPAL FEATURES

Using the potential profiles obtained for each spin component of each type of carrier in Sec. V, we can solve numerically the corresponding Schrödinger equation: the results are given now and compared to experimental data. In addition we discuss in this section several aspects of the model: the choice of the band offset value, the mathematical form of the composition profile, and the influence of the intrinsic magnetic correction present even at a perfectly abrupt interface.

A. Magnitude of the Zeeman effect

The results of the calculations can be directly compared with experimental data; for the quantum wells of sample M097 this has been done in Fig. 1. Another way of presenting the data is shown in Fig. 10. We chose to represent quantum-well exciton Zeeman splitting as a function of the barrier splitting, since the magnetic variations of the band offsets are proportional to this splitting. As pointed out in Ref. 13, the following conclusions can be drawn from these results

(i) Interface broadening leads to a dramatic increase of quantum-well Zeeman splittings, for two reasons: first, we dilute the magnetic ions in the interface region, decreasing the influence of ion-ion interaction and therefore increasing their magnetization[39] and in turn the band splittings; second, a broadened interface profile makes carrier penetration easier. In particular, the striking fact that the QW1 splittings are greater than the barrier splittings is reproduced by the calculations.

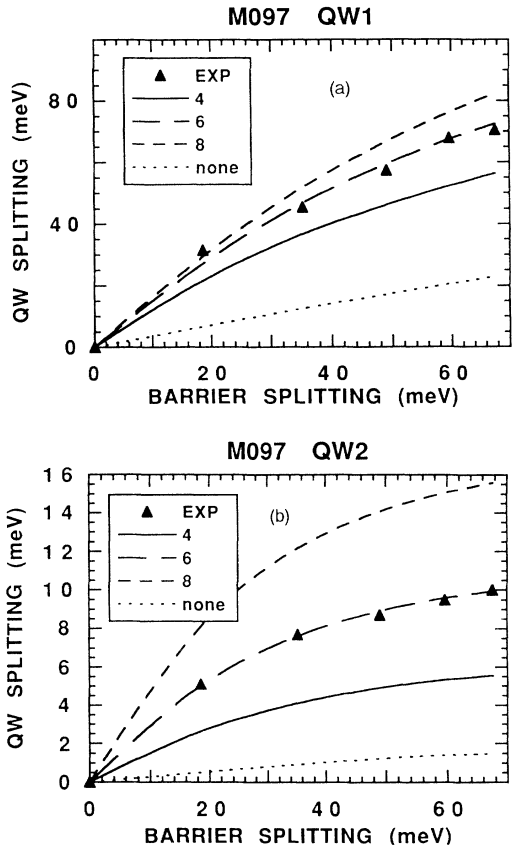

FIG. 10. Calculated (lines) and experimental (points) e^1h^1 exciton Zeeman splitting vs heavy hole barrier exciton splitting for sample M097: (a) QW1 (w = 17 Å) and (b) QW2 (w=66 Å). Values of intermixing length indicated in Å.

(ii) Whereas for a perfect quantum well [without intermixing, $l_0 = 0$ in Fig. 10(a)] the Zeeman splitting is a slightly superlinear function of the barrier splitting, interface mixing makes it sublinear. This results from a contribution of the lower Mn content in the interface and therefore a tendency to saturate faster with magnetic field (lower T_0 value). The experimentally observed sublinear dependence supports the image presented here, consistently with previous qualitative observations.[18,19]

We must stress that using a single adjustable parameter (intermixing length l_0) we are able to describe both the absolute values and field dependence of the Zeeman splitting in two different quantum wells of sample M097. In spite of very different well widths (by a factor of 4) and splitting values (by a factor of 7) we obtain very close values of the fitting parameter for both wells, l_0 = 6.1 Å and 5.6 Å in Table I.

B. Band offset

Measurements of Zeeman splittings have been often used in attempts to determine the valence band offset in CdTe-$Cd_{1-x}Mn_xTe$. Two questions arise: (i) Is the present study of interface dilution sensitive to the reparti-

tion of the band gap which is assumed in the calculation? (ii) How does interface dilution affect various estimates of the valence band offset?

In order to examine the sensitivity of the calculated results to band offsets, we present in Fig. 11 curves calculated for three valence band offset values: 0.2, 0.3, and 0.4 of the total band gap difference. Results for the narrower QW1 [Fig. 11(a)] do not depend significantly on the band offset, enabling us to determine the intermixing length independently of possible uncertainty in the band offset value. In case of QW2, where the valence band offset value influences the calculated Zeeman splitting, any realistic value (even α=0.2) leads to much lower splittings than the experimental ones if intermixing is neglected.

A detailed calculation reported by Chang *et al.*[16] yields Zeeman splittings consistent with their experimental data under the assumption of a very small valence band offset (1/14 of that of the conduction band). That results in a strong asymmetry of the computed Zeeman shifts in σ^+/σ^- polarizations (1:2), in contrast with the experiment. Such an asymmetry has been indeed observed, e.g., in a ZnSe/(Zn,Mn)Se system[10] possessing negligible valence band offset. Such a large asymmetry does not appear if the enhanced Zeeman effect is due to interface dilution. The other extreme value of the valence band offset, $\alpha = 0.46$, has been reported by Halsall *et al.*,[27] who deduce it from electron spin flip Raman scattering in multiple quantum wells. Given our results, it is easy to explain the difference: interface mixing strongly enhances the Zeeman splitting of the band states. Depending on whether the experiment primarily detects the valence band splitting (excitonic magneto-optics) or the conduction band splitting (spin flip Raman scattering), an analysis neglecting interface effects will tend to artificially decrease the offset of the carrier in question in order to increase its sensitivity to the barrier splitting. Therefore one can expect an overestimation of the value of relative valence band offset α for spin flip measurements[27] and an underestimation for excitonic Zeeman splitting measurements.[16]

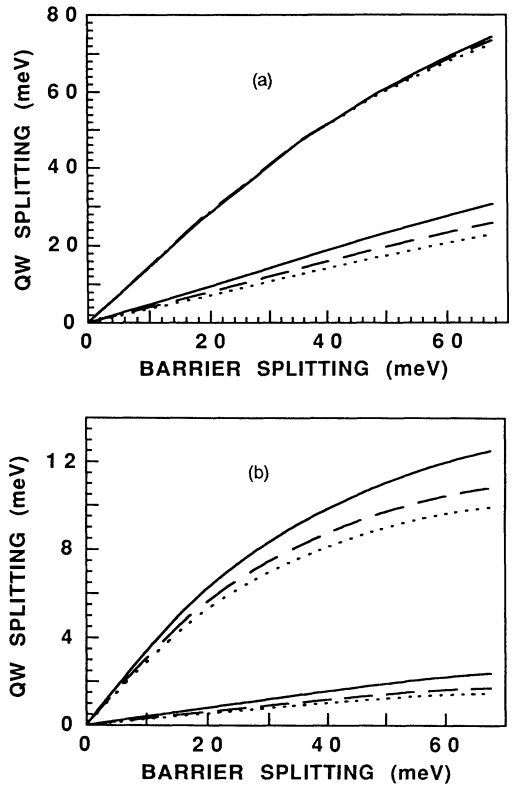

FIG. 11. Zeeman splittings calculated for quantum wells QW1 (a) and QW2 (b) of sample M097 for several values of relative valence band offset (solid line, $\alpha = 0.2$; dashed line, $\alpha = 0.3$; dotted line, $\alpha = 0.4$), plotted versus barrier heavy hole exciton splitting. Exponential profile with intermixing length 6 Å (upper curves) and square quantum well (lower curves).

Of course these interface effects will be larger in heterostructures with large manganese concentration in the barriers. This explains the unusual variation of the valence band offset with the Mn concentrations shown by Kuhn-Heinrich *et al.*[28] At small Mn concentration the interface effects are smaller but then the type I–type II transition of the $-3/2$ heavy hole potential profile is approached at moderate magnetic fields and the accompanying variation of the exciton binding energy has to be carefully taken into account.[41] It is interesting to note that valence band offsets determined using a method less sensitive to interface effects, i.e., the analysis of the light-heavy hole splitting converge to a value α in the range 0.3–0.4, whatever the Mn concentration.[41,42]

Finally in Fig. 12 we give an example of fitting the data of Ref. 43 using the present model. Using a valence band offset α equal either to 0.2 or to 0.4 we assign unambiguously the lines observed at 1692 and 1735 meV (see Fig. 1 of Ref. 43) to e_1h_3 and e_2h_2 excitons, respectively. As shown in Fig. 12, once again a good agreement is obtained if one introduces interface dilution (with a value of the interface width, $l_0 = 7$ Å, quite similar to those of Table I) and an intermediate value of the valence band offset (α=0.3). Some other recent papers consider excited states of $CdTe/Cd_{1-x}Mn_xTe$ quantum wells; Harrison *et al.*[20] express the opinion that a simultaneous analysis of the ground state and of excited states of the quantum-well exciton is a good way to determine the interface broadening. While not rejecting that idea, we must stress that the ground state, whose penetration depth is the smallest, is the best suited to study interface magnetization: note, however, that in Fig. 12 the agreement is quite good for all the electron-heavy hole transitions.

C. Composition profile

To choose the intermixing profile that best matches the reality we may consider two principal mechanisms: interdiffusion and segregation. In Ref. 13 we chose an error function profile, having no direct experimental evidence allowing us to determine its shape. In the present work we are able to shed some light on this problem. Bulk-type interdiffusion, commonly assumed to pro-

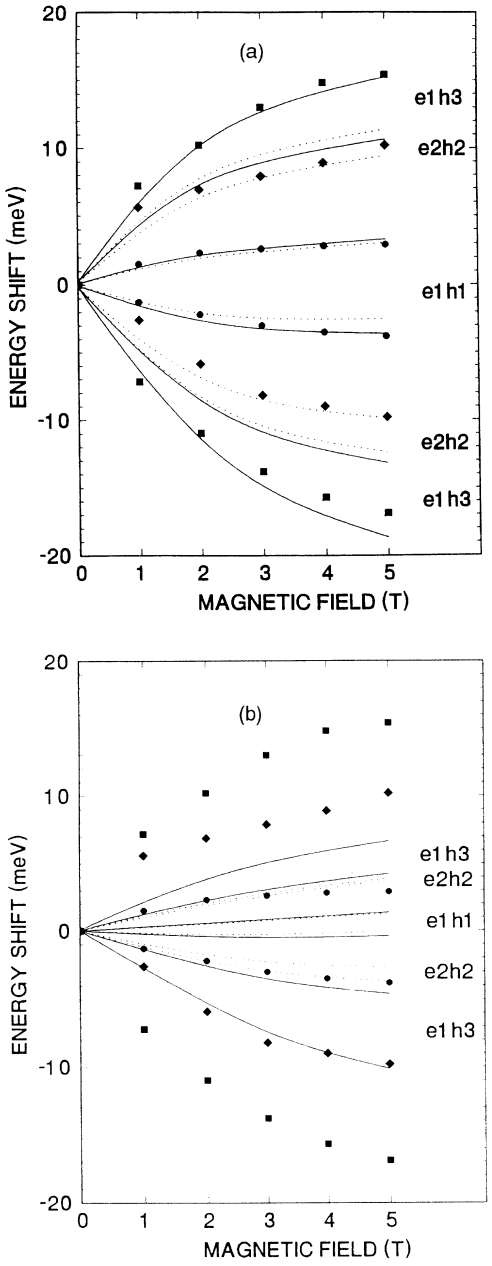

FIG. 12. Experimental data of Kuhn-Heinrich *et al.*[43] and our simulation results. Solid line, $\alpha = 0.2$; dotted line, $\alpha = 0.4$. Exponential profile with intermixing length 7 Å (a); no interface broadening (b).

duce an error function profile, may be eliminated in our case since annealing experiments show that diffusion in $CdTe/Cd_{1-x}Mn_xTe$ superstructures starts at temperatures higher than those presently used in the growth process. Moreover, bulk-type interdiffusion would lead to a symmetrical profile, with both interfaces exhibiting the same profile. Segregation, which would produce an approximately exponential profile,[25] is one possible mechanism of the observed intermixing. An important feature of the exponential profile is its asymmetry relative to the growth direction (see Fig. 4). The evidence of an asymmetric quantum-well profile is given by the magnetoreflectivity measurements on samples M336 and M340 containing each a CdTe well with one magnetic ($Cd_{1-x}Mn_xTe$) and one nonmagnetic (CdZnTe) barrier. The principal difference between the two structures is the order of growth of the two barriers. Any significant difference in the Zeeman splitting between the two samples proves that for the exciton localized in the quantum well, the $CdTe/Cd_{1-x}Mn_xTe$ interface is different from the $Cd_{1-x}Mn_xTe/CdTe$ one. The experimental magnetoreflectivity data presented in Fig. 2 for the two samples show a difference by a factor of 3 in the Zeeman splittings, proving beyond any doubt a strong asymmetry of the quantum-well profile. A complete analysis of results obtained on asymmetric samples is out of the scope of the present paper; fitting the experimental data for sample M336 with an exponential profile, we obtain an intermixing length $l_0 = 4.7$ Å (Fig. 13). The measured values of the splittings for sample M340 are small, and we expect a larger relative contribution of the intrinsic interface effect and of the direct Zeeman effect. This does not allow us to deduce an l_0 value. The simulation performed for the sample M340, Fig. 13(b), shows that the experimental results are consistent with an l_0 value close to 4.7 Å i.e., the value determined for M336. The steep initial rise of the inverse exponential interface profile in this case (M340) makes the influence of the intermixing very small. An additional argument supporting the choice of the exponential profile is a better agreement

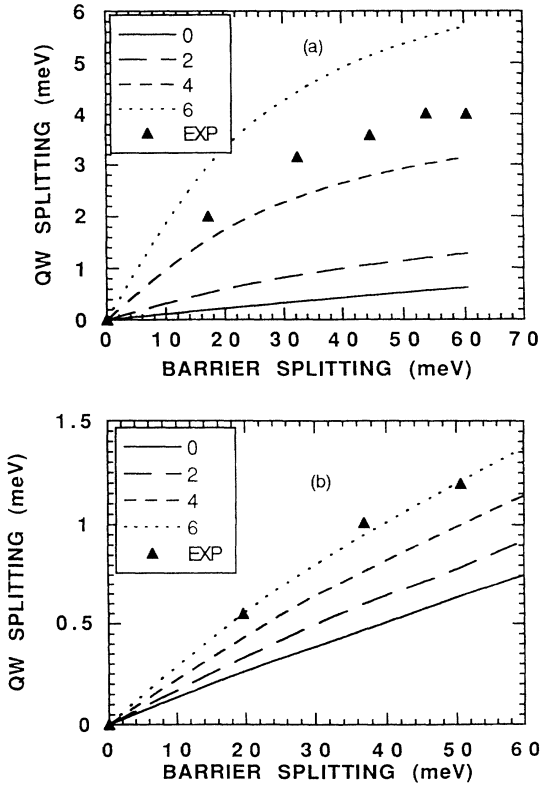

FIG. 13. Calculated (lines) and experimental (points) e^1h^1 exciton Zeeman splitting vs heavy hole barrier exciton splitting for samples M336 (a) and M340 (b). Values of intermixing length indicated in Å.

between the intermixing range values obtained for both quantum wells of sample M097. While in Ref. 13, using the error function profile, we obtained 4.3 Å and 6 Å for the two quantum wells, the exponential profile gives much closer values 5.6 Å and 6.1 Å, respectively (see Table I). Discussing the profile choice, we may consider other possibilities which were recalled at the beginning of Sec. IV. Some of them (short-scale surface roughness during growth of $Cd_{1-x}Mn_xTe$, enhanced diffusion close to the surface, Mn depletion at the $Cd_{1-x}Mn_xTe$ surface etc.) can be tentatively described with a broad Gaussian profile at the inverted (CdTe on $Cd_{1-x}Mn_xTe$) interface and a sharper one at the direct ($Cd_{1-x}Mn_xTe$ on CdTe) interface. The influence of such interface broadening on the magnitude of the Zeeman effect has been calculated and differs little from the case of an exponential profile.

Another profile could be introduced in case of two-dimensional (2D) growth and would contain one monolayer of an intermediate composition between the barrier and the well. The composition of that layer (the parameter of the profile) would correspond to the fraction of an atomic layer of the barrier grown before switching the effusion cells to grow the well, or to the incomplete metal coverage of the growing surface. Such a profile (which cannot be defined in the same way as those from Table II) can be defined as a combination of the "layer-by-layer" calculation with zero interface length discussed in Sec. VII below. Attempts to fit the data, e.g., for QW1 of sample M097, show that whatever the value of the parameter, the calculated splittings are at least five times too small. However, such profiles could represent an upper limit to the abruptness of interfaces realized without attempting to modify the stoichiometry of the growing surface (surface reconstructions) and its shape (island size).

The present discussion is based on the assumption of a continuous profile, while at the present stage it is difficult to separate the influence of interface roughness. Therefore in our opinion no definitive conclusions on the shape of the intermixing profile can be reached yet. Combining different methods to characterize interfaces of the same samples should be the best way to handle this problem. In spite of this difficulty, our conclusions about the physical mechanism of the enhancement of the Zeeman effect remain valid, as they are not very sensitive to the detailed profile shape.

D. Estimation of the intrinsic magnetic correction

As we pointed out previously, the magnetic ions in an atomic plane in the interface will have in general a different number of magnetic neighbors than in a bulk crystal of the same composition as that of the layer. If we want to count only the nearest neighbors of the cation sublattice, for the (001) growth direction, each cation will have four neighbors in its atomic plane and four in each of the two adjacent planes. We cannot therefore expect that local magnetization will correspond precisely to the local alloy composition; it must be also influenced by the adjacent atomic layers. This fact will modify the observed magneto-optical results by a value that we shall call the interface magnetic correction (intrinsic, as opposed to the dilution effect). For a quantitative analysis, it is very important to know the relative contribution of intermixing and interface magnetic correction to the final result. The results discussed above, obtained on samples M336 and M340 (Figs. 2 and 13) supply a striking direct proof not only of the asymmetry of the quantum-well profile, but also of the relatively small importance of the interface magnetic correction. An estimate of this correction can be obtained by defining an effective alloy composition

$$x_{\text{eff}}(z) = [x(z) + x(z-a) + x(z+a)]/3 \qquad (9)$$

that is the composition of a bulk crystal in which the ions have the same number of nearest magnetic neighbors as those in our atomic layer [a denotes the layer thickness, equal to half of the lattice constant; this neighbor count is valid for nearest neighbors only and (001) growth direction]. Now we shall assume that each ion in the interface is aligned by an external magnetic field in the same way as in a bulk crystal of composition x_{eff}. The local magnetization will be thus equal to the bulk magnetization corresponding to a composition x_{eff}, multiplied by the ratio x/x_{eff} (to account for a different density of magnetic ions). The same will hold for the splittings of the bands, i.e.,

$$\Delta E_{\text{corrected}}(x) = \Delta E(x_{\text{eff}}) \frac{x}{x_{\text{eff}}} .$$

Figure 14 shows heavy hole potentials in a field of 5 T, calculated for the parameters of the thinner quantum-well of sample M097. The potential splitting, i.e., the difference of potential values for the two hole spin orientations, is presented below. We see a strong enhancement of the splitting in the interface regions, caused by the dilution of magnetic ions (dotted line, no intrinsic magnetic correction). The splitting at the left interface is further enhanced by the magnetic correction (continuous line).

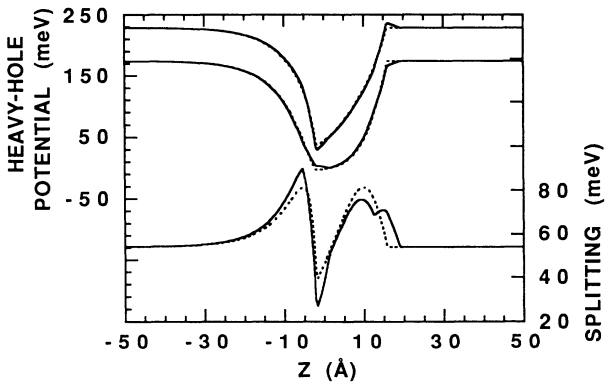

FIG. 14. Top: Heavy hole potentials for both (±3/2) hole spin orientations in a field of 5 T, calculated for the parameters of the thinner quantum-well of sample M097 ($l0$ = 5.6 Å, w=17 Å). Below, the difference of the two potentials. Dashed line, no interface magnetic correction; solid line, with interface magnetic correction.

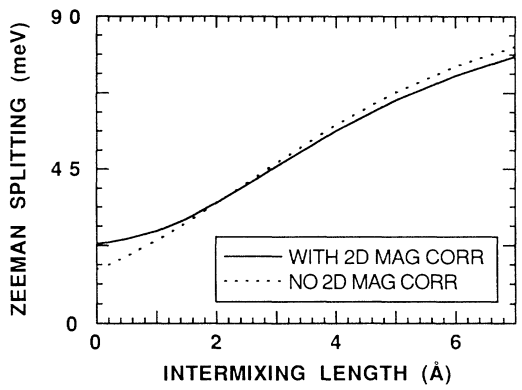

FIG. 15. Zeeman splitting for e^1h^1 transition at a magnetic field of 5 T, calculated with (continuous) and without (dashed line) interface magnetic correction, as a function of intermixing length. Exponential profile, $\alpha = 0.4$, parameters of QW1 of sample M097 (w=17 Å).

We notice also an additional peak of the splitting at the right interface, resulting from a smaller number of magnetic neighbors of the ions from the first atomic layer of the barrier. However, there exists a region in the right interface where introduction of the magnetic correction leads to a decrease of the splitting. This is due to a bigger number of magnetic neighbors of the ions in this part of the interface, compared to a bulk alloy of the local composition. It is clear, from the expression of x_{eff}, that we can expect such a decrease in regions of positive second derivative of the profile function.

Figure 15 shows how these two opposite effects combine to produce a 2D magnetic correction to the interband transition energy for the thinner well, QW1, of sample M097. While at small intermixing range values the correction causes a rather strong increase of the Zeeman splitting, for higher intermixing length values it produces a slight decrease of the Zeeman splitting . For the parameters of the samples discussed in the present work (except M340), our estimate of the 2D magnetic correction is always small enough to be neglected. These estimates are based on a local model, which takes into account only the change in the number of nearest neighbors without any reference to a correlation length of the magnetic order: on the other hand results of sample M340 clearly show that for such alloy compositions and layer thicknesses the 2D magnetic corrections are experimentally small. They may become important for very thin magnetic barriers and/or very high Mn concentration.

VII. FACTORS INFLUENCING THE PRECISION OF THE DESCRIPTION

The nominal well width values of our samples have a limited precision (usually to a fraction of one atomic layer). In a certain range of parameters (large Mn mole fraction in the barriers and small intermixing range), a change of the well width mainly shifts the absolute energy of the optical transitions, while the intermixing length primarily influences the Zeeman splitting. This may not be quite true in a general case. In particular, for parameters close to those of quantum wells of samples M162, M177, and M178, such a separation does not occur. We often have to slightly adjust the well width to fit the zero-field exciton energy: this does not imply that we consider all the fitting procedure to be accurate at the scale of the meV, but it allows to compare the intermixing length in samples with different but similar quantum-well parameters (e.g., M162, M177, M178 in Table I).

Besides the exchange-mediated Zeeman splittings, we always have the direct influence of the magnetic field on the carriers, producing usual (direct) Zeeman splittings, diamagnetic shift of the excitonic energy and, in sufficiently strong magnetic field, Landau quantization. All these effects in the magnetic field range used in this work are below 1 meV for 1s exciton states as shown by magneto-optical measurements on CdTe-$Cd_{1-x}Zn_xTe$ multiple quantum wells.[44] Therefore if the observed splittings are important compared to 1 meV (e.g., the case of sample M097) we can neglect the direct effects. In the opposite case (e.g., sample M340), we must take them into account.

In the final fits we take into account the exciton binding energies and their variation with magnetic field. For the structures described in this paper (with high Mn concentrations in the barriers), the magnetic variation of the binding energy is small and the accuracy of their calculation (see above) is sufficient. For structures with small Mn concentration in the barrier the situation is quite different: the application of a magnetic field may induce a type I–type II transition for the $-3/2$ hole potential, resulting in a drastic variation of the corresponding σ^+ exciton binding energy.[33,41] A reliable determination of that variation should take into account valence band mixing effects which would imply complicated numerical calculations. This is one of the reasons why our technique is not suitable for the characterization of interfaces in heterostructures with small Mn concentrations.

In our calculations we use, in the spirit of the effective mass method, a continuous model for the quantum-well potential, whereas the real structures have of course atomic layer structure. To test the validity of our approach, we performed some test calculations in a discrete model, where we replaced the continuous potential by a steplike function, calculated on a grid of atomic layer distances. Introducing a grid we face an additional degree of freedom, having to choose the origin of the z axis related to the grid. Physically, it corresponds to the choice of the moment of switching the sources in the MBE process. The results of the test calculation as a function of that displacement, performed for parameters corresponding to one of the quantum wells of sample M097, show a certain variation in the calculated energies, less than 0.3 meV, which does not significantly modify any conclusions we may draw from the analysis of our results. Furthermore, the energy averaged over possible values of the z origin displacement is with an excellent accuracy equal to the value obtained from the continuous model.

VIII. APPLICATION OF THE METHOD

In Fig. 16 we present results obtained for the series of three samples grown at different temperatures. It is interesting to note that, in spite of some differences in the quantum-well width and the composition of the barriers (see Table I), it was possible to choose independent y-axis scales for each sample in such a way that the curves calculated for the same intermixing length values coincide to a good approximation. Thus the relative position of experimental points on such a plot allows to compare the intermixing values of different samples. We can see that the intermixing length increases with growth temperature in the range 250 °C to 310 °C and that the magneto-optical method detects important differences between samples grown at different temperatures. Even using a simplified version of the method, while we cannot guarantee precise values of the determined intermixing length, we can detect its variation with enough sensitivity to optimize the growth process. Besides growth temperature, the influence of other growth parameters may be examined, e.g., growth interruptions, relative values of fluxes of the effusion cells, etc. We have performed such a study on a series of samples; it will be reported in a future publication.

In view of the results of this work extreme caution must be applied when looking for 2D magnetic effects in thin layers of magnetic semiconductors. Although both intuitive arguments and simulation results allow us to expect dramatic effects in very thin layers, any realistic interface mixing will drastically modify the expected results. Figure 14 shows that intermixing may do this al-

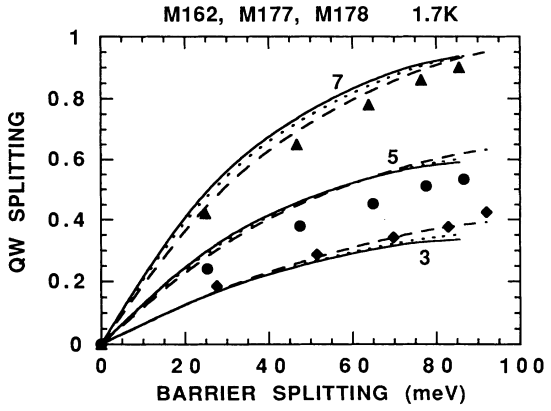

FIG. 16. Calculated (lines) and experimental (points) e^1h^1 exciton Zeeman splitting vs heavy hole barrier exciton splitting for samples M162, M177, and M178. Respective values of full scale energy for the three samples have been chosen to obtain approximate coincidence of the theoretical curves in spite of small variations in quantum-well width and barrier composition; see Table I. The intermixing length is indicated in Å. Sample M162 (grown at 310 °C): triangles = experimental, dotted line = calculation, full scale = 10 meV; sample M177 (grown at 280 °C): circles = experimental, dashed line = calculation, full scale = 13.6 meV; sample M178 (grown at 250 °C): diamonds = experimental, solid line = calculation, full scale = 14.5 meV.

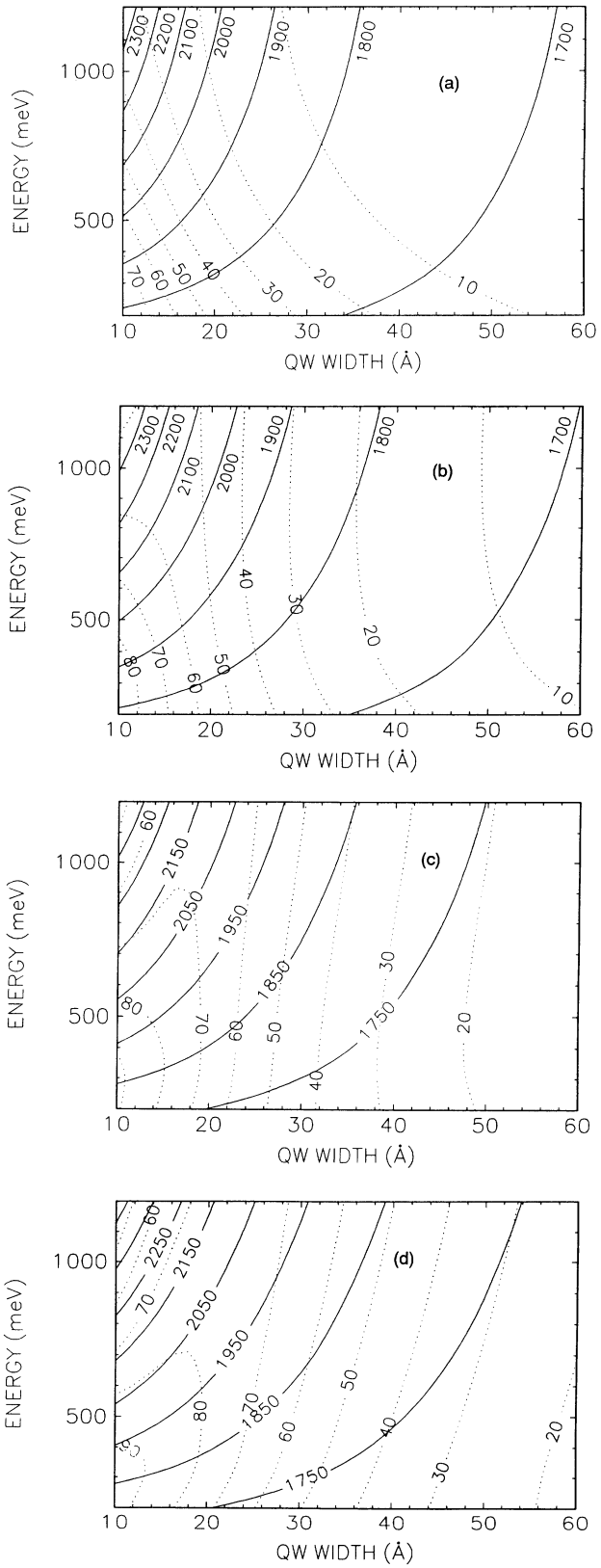

FIG. 17. Grids of constant zero field energy (solid line) and Zeeman splitting (dotted line) values calculated for e^1h^1 excitons and represented in QW width–E_x plane for four intermixing length values: 2 Å (a), 4 Å (b), 6 Å (c), and 8 Å (d). Energies in meV. Calculation parameters: $\alpha = 0.4$, $T = 1.7$ K, $B = 5$ T, exponential profile.

ready at intermixing range values of the order of 1 Å and in our experiments we never encounter such low values (see Table 1). Therefore in any 2D magnetic studies on $Cd_{1-x}Mn_xTe$ or similar materials the growth procedure must be carefully optimized to produce the sharpest possible interface, and a detailed analysis must include the influence of interface mixing.

Several problems discussed above influence the useful range of the application of the magneto-optical method of interface characterization. If we want to have a reliable method and a simple (and fast) numerical procedure, we will be interested in getting rid of a maximum number of complications. To do this we should satisfy three conditions: (i) stay away from type I–type II transitions (complicated and unreliable exciton binding energy calculations), (ii) have the Zeeman splittings large compared to 1 meV (direct Zeeman effect), (iii) have a sufficiently precise knowledge of the quantum-well width, for instance through RHEED oscillations, or otherwise be assured that the two adjustable parameters (well width and intermixing length) are not correlated. The first condition will be fulfilled if we use barriers of E_x above 300 meV (Mn mole fraction above 0.2; see Fig. 9). From Figs. 17(a)–17(d) it is clear that the second condition is satisfied if we use barrier compositions above 15% and quantum-well widths below 60 Å. An idea on the third condition can be obtained by calculating a grid well width—intermixing length in the Zeeman splitting—zero field energy plane for various compositions of the barriers: determination of the two quantum-well parameters at low concentration of Mn in the barriers will be much less precise because of their stronger correlation (at constant intermixing length the Zeeman splitting shows large variations with the quantum-well width). Summarizing, we should try to use Mn concentrations in barriers at least 20% and well width below 50 Å in order to be able to use the simplest version of the method. Stepping outside the safe area requires a more careful (and cumbersome) analysis of the results.

Figure 17 can also be used to get a preliminary estimate of intermixing without making specific numerical calculations. We find the point corresponding to the zero-field energy and Zeeman splitting values, and read from the plot the barrier energy (E_x). This we repeat for figures calculated for different intermixing range values and we chose the one where the read E_x value agrees best with the experimental one (we know it from the free exciton energy of the barrier material). Of course, interpolation may be useful.

IX. CONCLUSIONS

We have presented a coherent description of magneto-optical splittings of excitons in $CdTe/Cd_{1-x}Mn_xTe$ quantum wells. We have shown that the observed strong enhancement of the Zeeman splittings results primarily from dilution of magnetic ions in interfaces and allows us to measure the interface mixing range. We pointed out possible sources of errors which may be introduced by neglecting the interface mixing in determining band offsets and in studies of 2D magnetic properties. We have shown that the quantum-well profiles are strongly asymmetric and that the influence of intrinsic interface magnetism in simple wells is small within the studied range of experimental conditions. Although the exact shape of the interface profile is not yet known (we chose the exponential profile as the most probable), our method gives quite precise information allowing us to compare samples grown under various conditions. Any future improvement of the knowledge of interface shape will probably introduce only a slight scaling of our results. The presented method of interface characterization is sensitive primarily to short range order of magnetic ions and therefore requires complementary characterization tools when information on long range interface perturbation is important.

ACKNOWLEDGMENTS

We thank Dr. R. Planel for suggesting the study of asymmetric structures. One of us (J.G.) acknowledges support from CNRS. We thank R. Romestain and P. Peyla for their contribution to the initial part of this work, R. Cox, Le Si Dang, H. Mariette, and J.E. Nicolls for fruitful discussions, and R. Legras for technical assistance. This work was performed within the Centre National de la Recherche Scientifique–Commisariat à l'Energie Atomique group "Microstructures de Semiconducteurs II-VI". The Laboratoire de Spectrométrie Physique is laboratoire associé au Centre National de la Recherche Scientifique.

* On leave from Warsaw University, Poland.

[1] R.K. Kopf, E.F. Schubert, T.D. Harris, and R.S. Becker, Appl. Phys. Lett. **58**, 631 (1991).

[2] D. Gammon, B.V. Shanabrook, and D.S. Katzer, Phys. Rev. Lett. **67**, 1547 (1991).

[3] D. Bimberg, J. Christen, T. Fukanaga, H. Nakashima, D.E. Mars, and J.N. Miller, J. Vac. Sci. Technol. B **5**, 1191 (1987).

[4] B. Jusserand, F. Molot, J.-M. Moison, and G. Le Roux, Appl. Phys. Lett. **57**, 560 (1990).

[5] T. Noda, M. Tanaka, and H. Sakaki, Appl. Phys. Lett. **57**, 1651 (1990).

[6] A. Krol, H. Resat, C.J. Sher, S.C. Woronick, W. Ng, Y.H. Kao, T.L. Cole, A.K. Green, C.K. Lowe-Ma, T.-W. Nee, and Victor Rehn, J. Appl. Phys. **69**, 949 (1991).

[7] A. Ourmazd, D.W. Taylor, J. Cunningham, and C.W. Tu, Phys. Rev. Lett. **62**, 933 (1989).

[8] P. Bogusławski, in *Proceedings of the XXI International Conference Physics Semiconductors*, Beijing, 1992, edited by Ping Jiang and Hou-Zhi Zheng (World Scientific, Sin-

gapore, 1992), p. 397.
[9] J.K. Furdyna, J. Appl. Phys. **64**, R29 (1988) and references therein.
[10] X. Liu, A. Petrou, J. Warnock, B.T. Jonker, G.A. Prinz, and J.J. Krebs, Phys. Rev. Lett. **63**, 2280 (1989).
[11] W.C. Chou, A. Petrou, J. Warnock, and B.T. Jonker, Phys. Rev. Lett. **67**, 3820 (1991).
[12] N. Dai, H. Luo, F.C. Zhang, N. Sammarth, M. Dobrowolska, and J.K. Furdyna, Phys. Rev. Lett. **67**, 3824 (1991)
[13] J.A. Gaj, C. Bodin-Deshayes, P. Peyla, J. Cibert, G. Feuillet, Y. Merle d'Aubigné, R. Romestain, and A. Wasiela, Ref. 8, p. 1936.
[14] See, e.g., J.A. Gaj, in *Semiconductors and Semimetals,* edited by J.K. Furdyna and J. Kossut (Academic, Boston, 1988), Vol. 25, p. 275.
[15] W. Ossau, S. Fischer, and R.N. Bicknell-Tassius, J. Cryst. Growth **101**, 905 (1990).
[16] S.-K. Chang, A.V. Nurmikko, J.-W. Wu, L.A. Kolodziejski, and R.L. Gunshor, Phys. Rev. B **37**, 1191 (1988).
[17] N. Pelekanos, Q. Fu, J. Ding, W. Walecki, A.V. Nurmikko, S.M. Durbin, J. Han, M. Kobayashi, and R.L. Gunshor, Phys. Rev. B **41**, 9966 (1990).
[18] A. Wasiela, Y. Merle d'Aubigné, J.E. Nicholls, D.E. Ashenford, and B. Lunn, Solid State Commun. **76**, 263 (1990).
[19] R. Meyer, M. Hirsch, G. Schaack, A. Waag, and R.-N. Bicknell-Tassius, Superlatt. Microstruct. **9**, 165 (1991).
[20] P. Harrison, W.E. Hagston, and T. Stirner, Phys. Rev. B **24**, 16 404 (1933).
[21] D.D. Awschalom, J.M. Hong, L.L. Chang, and G. Grinstein, Phys. Rev. Lett. **59**, 1733 (1987).
[22] W.J. Ossau and B. Kuhn-Heinrich, Physica B **184**, 422 (1993).
[23] A. Twardowski, H.J.M. Swagten, W.J.M. de Jonge, and M. Demianiuk, Phys. Rev. B **36**, 7013 (1987).
[24] P.H. Jouneau, A. Tardot, G. Feuillet, H. Mariette, and J. Cibert, Inst. Phys. Conf. Ser. **134**, 329 (1993).
[25] J.M. Moison, C. Guille, F. Houzay, F. Barthe, and M. Van Rompay, Phys. Rev. B **40**, 6149 (1989).
[26] S. Tatarenko, F. Bassani, J.C. Klein, K. Saminadayar, J. Cibert, and V.H. Etgens J. Vac. Sci. Technol (to be published).
[27] M.P. Halsall, D. Wolverson, J.J. Davies, D.E. Ashenford, and B. Lunn, Solid State Commun. **86**, 15 (1993).
[28] B. Kuhn-Heinrich, W. Ossau, M. Popp, E. Bangert, A. Waag, and G. Landwehr, Ref. 8, p. 923
[29] D.G. Thomas, J. Appl. Phys. (suppl.) **32**, 2298 (1961); M. Zigone, H. Roux-Buisson, H. Tuffigo, N. Magnéa, and H. Mariette, Semicond. Sci. Technol. **6**, 454 (1991); B. Gil and D.J. Dunstan, *ibid.* **6**, 428 (1991); Y. Merle d'Aubigné, H. Mariette, N. Magnéa, H. Tuffigo, R.T. Cox, G. Lentz, Le Si Dang, J.L. Pautrat, and A. Wasiela, J. Cryst. Growth **101**, 650 (1990).
[30] R.D. Greenough and S.B. Palmer, J. Phys. D **6**, 587 (1973).
[31] P. Maheswaranathan, R.J. Sladek, and U. Debska, Phys. Rev. B **31**, 5212 (1985).
[32] P. Peyla, Ph.D. thesis, Université Grenoble I, 1992; P. Peyla, Y. Merle d'Aubigné, A. Wasiela, R. Romestain, H. Mariette, M.D. Sturge, N. Magnéa, and H. Tuffigo, Phys. Rev. B **46**, 1557 (1992).
[33] E. Deleporte, J.M. Berroir, G. Bastard, C. Delalande, J.M. Hong, and L.L. Chang, Phys. Rev. B **42**, 5892 (1990).
[34] G. Peter, E. Deleporte, G. Bastard, C. Delalande, B. Gil, J.M. Hong, and L.L. Chang, J. Lumin. **52**, 147 (1992)
[35] R.P. Leavitt and J.W. Little, Phys. Rev. B **42**, 11 774 (1990).
[36] C. Neuman, A. Nöthe and N.O. Lipari, Phys. Rev. B **41**, 6082 (1988); Le Si Dang, G. Neu, and R. Romestain, Solid State Commun. **44**, 1187 (1982) give slightly different values, the conclusions on the interface effect do not depend on the chosen set of parameters.
[37] *Numerical Data and Functional Relationships in Sciences and Technology*, edited by O. Madelung, Landolt-Bornstein, New Series Group III Vol. 17a (Springer-Verlag, Berlin, 1982).
[38] D. Coquillat and J.P. Lascaray (unpublished).
[39] J.A. Gaj, R. Planel, and G. Fishman, Solid State Commun. **29**, 435 (1979).
[40] J.A. Gaj, Acta Phys. Pol. A **73**, 463 (1988).
[41] A. Wasiela, P. Peyla, Y. Merle d'Aubigné, J.E. Nicholls, D.E. Ashenford, and B. Lunn, Semicond. Sci. Technol. **7**, 571 (1992).
[42] B. Kuhn-Heinrich, W. Ossau, T. Litz, A. Waag, and G. Landwehr, J. Appl. Phys. (to be published).
[43] B. Kuhn, W. Ossau, A. Waag, R.N. Bicknell-Tassius, and G. Landwehr, J. Cryst. Growth **117**, 871 (1992).
[44] K. Kheng, R.T. Cox, Y. Merle d'Aubigné, F. Bassani, K. Saminadayar, and S. Tatarenko, Phys. Rev. Lett. **71**, 1752 (1993); R.T. Cox (private communication).